Pharmacogenomics and Personalized Medicine

Dovepress

open access to scientific and medical research

Open Access Full Text Article

ORIGINAL RESEARCH

PUS1 May Be a Potential Prognostic Biomarker and Therapeutic Target for Hepatocellular Carcinoma

Chenlu Lan[1,2,*], Xinlei Huang[1,2,*], Xiwen Liao[1,2], Xin Zhou[1,2], Kai Peng[1,2], Yongguang Wei[1,2], Chuangye Han[1,2], Tao Peng[1,2], Jianyao Wang[3], Guangzhi Zhu[1,2]

[1]Department of Hepatobiliary Surgery, The First Affiliated Hospital of Guangxi Medical University, Nanning, Guangxi Zhuang Autonomous Region, People's Republic of China; [2]Key Laboratory of High-Incidence-Tumor Prevention & Treatment (Guangxi Medical University), Ministry of Education, Nanning, 530021, People's Republic of China; [3]Department of General Surgery, Shenzhen Children's Hospital, Shenzhen, Guangdong Province, People's Republic of China

*These authors contributed equally to this work

Correspondence: Guangzhi Zhu, Department of Hepatobiliary Surgery, The First Affiliated Hospital of Guangxi Medical University, Nanning, 530021, Guangxi Zhuang Autonomous Region, People's Republic of China, Tel +86-771-5356528, Fax +86-771-5350031, Email zhuguangzhi0792@hotmail.com; Jianyao Wang, Department of General Surgery, Shenzhen Children's Hospital, Lianhua District, Shenzhen, 518026, Guangdong Province, People's Republic of China, Email yaozi66@126.com

Objective: The mechanisms of pseudouridine synthase (PUS) are not definite in hepatocellular carcinoma (HCC), the objective of this study is to investigate the effect of PUS genes in HCC.

Materials and Methods: Differentially expressed and prognostic gene of PUS enzymes was identified based on The Cancer Genome Atlas (TCGA), International Cancer Genome Consortium (ICGC) and Gene Expression Profiling Interactive Analysis (GEPIA) databases. For the identified gene, pseudouridine synthase 1 (*PUS1*), was used for further research. The clinicopathological feature of *PUS1* was analyzed by Student's *t*-test. Prognostic significance was explored by Kaplan-Meier (KM) analysis and Cox proportional hazards regression model. Receiver operating characteristic (ROC) curve was applied to appraise diagnostic and prognostic value. The Database for Annotation, Visualization, and Integrated Discovery (DAVID) and Gene Set Enrichment Analysis (GSEA) were implemented to explore mechanism of *PUS1*. A Guangxi cohort was applied to verify differential expression. In vitro cell experiments were implemented to investigate the influence for proliferation, reactive oxygen species (ROS) level, migration, and invasion of HCC cells after a knockdown of *PUS1*.

Results: *PUS1* was significantly overexpressed in HCC tissues, and patients with high *PUS1* were related to unpromising clinicopathological features. Survival analysis revealed high *PUS1* expression was associated with a poor overall survival (OS) and 1 year-recurrence free survival (RFS), was an independent risk factor. Meanwhile, ROC curve showed that *PUS1* had a diagnostic and prognostic significance to HCC. Functional enrichment analysis implied that *PUS1* may be involved in metabolic pathways, mitochondrial function, non-alcoholic fatty liver disease (NAFLD), and some important carcinogenic pathways. Cell assays revealed that knockdown of *PUS1* significantly constrained the migration, proliferation, invasion and improved the ROS level of HCC cells.

Conclusion: *PUS1* may be a prognostic biomarker and a underlying treatment target for HCC.

Keywords: *PUS1*, pseudouridine synthase, poor prognosis, gene knockout, HCC

Introduction

Cancer brings a heavy burden to society, primary liver cancer has the seventh incidence and second mortality rates worldwide, about 75–85% of patients of primary liver cancer are HCC.[1] Primary prevention contributes to reduce the incidence of HCC. Early diagnosis and management can improve OS for HCC patients.[2] Currently, early detection of HCC still depends on ultrasonography and serum α-fetoprotein (AFP), yet the accuracy for early stage is not so satisfactory.[3] Therefore, substantial studies focus on seeking new biomarkers or tests which have a better diagnostic or prognostic value for HCC. Protein Induced by Vitamin K Absence or antagonist-II (PIVKA-II)[4] and AFP isoform L3 (AFP-L3)[5] have been applied for early detection and postoperative surveillance for HCC. The GALAD scoring system,

Received: 21 January 2023
Accepted: 31 March 2023
Published: 15 April 2023

consists of gender, age, AFP-L3, AFP and PIVKA-II, is a preferable approach for HCC detection.[6] In addition, many valuable biomarkers have emerged,[7] but the efficiency needs to be further determined clinically. Identification of novel biomarkers for diagnosis and surveillance contributes to guide the HCC treatment with a target mechanism.

The researches regard to modifications in cancer are progressively emerging, more and more evidence indicated that aberrant modifications were related to many cancers and may act as promising therapeutic targets.[8] For example, the N6-methyladenosine methylation has been reported to influence the tumor biological behavior through regulating some oncogenes or tumor suppressor genes,[9] and has become a focus in current cancer research.

Pseudouridylation functions as an abundant and ubiquitous RNA modification[10] through RNA-independent and RNA-dependent pathway.[11] The RNA-dependent way mainly relies on dyskerin (*DKC1*), non-histone protein 2 (*NHP2*), glycine-arginine-rich protein 1 (*GAR1*), and nucleolar protein 10 (*NOP10*).[12] These four proteins are essential catalysis of pseudouridylation and their genetic dysregulation can cause the ribosomal disease and cancer.[13–15] It was reported that their upregulated expressions in HCC were highly associated with poor prognosis.[16] RNA-independent pseudouridylation involves a crucial enzyme named PUS, which includes TruA, RluA, PUS10, TruB, and TruD families. The human homologs of PUS enzyme consist of *TRUB1, TRUB2, RPUSD1, RPUSD2, RPUSD3, RPUSD4, PUS1, PUS3, PUS7, PUS7L, and PUS10*.[17] The same as RNA-dependent mechanism, dysregulation of PUS enzymes also induces some congenital mitochondrial diseases and cancers.[8,18,19] For example, *PUS10* works as a mediator to affect the apoptosis of prostate cancer cells by tumor necrosis factor-related mechanism,[20] overexpression of *PUS7* activates the Wnt/β-catenin and PI3K/AKT/mTOR pathways to improve the proliferation and invasion of tumour cells.[21,22] Moreover, a study showed that some PUS enzymes play a diagnostic and prognostic role for HCC.[23]

However, the mechanisms of PUS enzymes keep obscure in HCC. Thus, the study aims to explore its clinicopathological value and potential functional mechanism to seek therapeutic target for HCC.

Materials and Methods

Data Sources

The RNA-seq (FPKM) data and clinicopathologic information of 370 HCC cases which included 370 HCC and 50 normal tissues were obtained from TCGA (https://cancergenome.nih.gov/). Meanwhile, we downloaded the microarray expression profiling and clinical information from the ICGC (https://dcc.icgc.org/projects/LIRI-JP) and the Gene Expression Omnibus (GEO) portal (https://www.ncbi.nlm.nih.gov/geo/). The ICGC cohort covers 240 HCC and 202 normal tissues, all cases come from Japan and about 75% patients had the HBV/HCV infection.[24] GSE14520 dataset was downloaded from GEO, which included 212 HBV-infected HCC patients of China.[25]

Identifying the Differential and Prognostic Gene

The mRNA expression level between HCC and normal tissues was compared to screen the differentially expressed genes via the Wilcoxon test. Every PUS enzymes gene was grouped into high and low groups base on the median of HCC expression respectively, then a univariate Cox survival analysis was utilized for seeking the prognostic genes. In addition, the differential expression and survive analysis were further validated by GEPIA database. Ultimately, we identified the *PUS1* gene as the differential and prognostic gene through above methods.

Exploring the Clinicopathological Features and Diagnostic Value of *PUS1*

In TCGA, ICGC, and GES14520 cohorts, Student's *t*-test was performed to compare the expression of HCC and normal tissues of *PUS1*, and explore the correlation of *PUS1* expression with clinicopathological factors. In addition, the diagnostic efficiency of *PUS1* was appraise by ROC analysis base on the expression of HCC and normal tissues. The expression data of TCGA and ICGC cohorts were converted with a $\log_2$ form to satisfy normal distribution.

Survival Analysis of *PUS1*

The grouping is same as described above. A univariate survival analysis, K-M analysis, was performed to determine the OS or RFS-related variables using the clinicopathological factors and *PUS1* group in TCGA, ICGC, and GSE14520

cohorts, the results of *PUS1* was next adjusted by those OS- or RFS-related variables in a Cox proportional hazards regression model. The joint-effect of OS or RFS-related variables with *PUS1* group was carried out to investigate the clinical value of *PUS1* further.

Prognostic Nomogram and Risk Score Model

OS-related clinical variables and *PUS1* group were used to structure the nomograms to forecast the survival rate of 1-, 3-, 5-year OS, and 1-year RFS in TCGA and GSE14520 cohorts, the conformance of realistic and predicted survival situation was checked by calibration curve.

The risk score of every patient was counted by the formula: risk score $=$(expression value of gene A)$\times\beta$A $+$ (expression value of gene B)$\times\beta$B $+ \ldots$(expression value of gene n)$\times\beta$n, where β is the regression coefficient.[26] Next, the patients of TCGA and GSE14520 cohorts were separated into two groups by the median of risk score, and we constructed a risk score model to intuitively display how *PUS1* expression impacted on the risk ranking, survival time, survival status and its prognostic value in HCC.

Functional Enrichment Analysis

A genome-wide correlation analysis of *PUS1* was completed to receive the co-expressed genes witch a Pearson correlation coefficient $|r| \geq 0.4$ and $p < 0.05$ in R software. Meanwhile, a "limma" package was used to mine the differential genes which had a |log2FC| value >1 and $p < 0.05$ between high risk and low risk groups. After that, the underlying functional mechanism of *PUS1* was explored on the DAVID (version 6.8, http://david.ncifcrf.gov) based on the co-expressed genes and differential genes of GSE14520 and TCGA cohorts, the results with a normalized p- <0.05 were defined as statistically significant.

To probe the potential function of *PUS1* in HCC as detailed as possible, we determined the enriched gene sets of high and low risk group in GSEA (v4.1.0, http://www.gsea-msigdb.org/gsea/index.jsp) with c2.all.v7.0.symbols.gmt and c5.all.v7.0.symbols.gmt files. A $p < 0.05$ and false discovery rate <0.25 were regarded to statistically significant.

Reverse Transcription-Quantitative PCR

For verifying the differential expression of *PUS1*, a total of 30 pairs of postoperative specimens which gathered from the First Affiliated Hospital of Guangxi Medical University (Guangxi cohort) were used to perform the Polymerase Chain Reaction (PCR). The RNA was extracted by the Trizol reagent (Invitrogen, USA) and reversely transcribed into cDNA by the PrimeScript™ RT reagent kit (Takara, China). The FastStart Universal SYBR® Green Master Mix (Roche, Germany) was then used to perform the PCR, we used the $2^{-\Delta\Delta CT}$ way to measure the relative mRNA expression of *PUS1*. In this experiment, the primer sequences of reference and target gene were severally as follows: *GAPDH*, forward: GTCAGCCGCATCTTCTTT, reverse: CGCCCAATACGACCAAAT. *PUS1*, forward: TATTCGGGCAAGGGCTACCA, reverse: CGTCAATCAGCCACACCTTC. All patients were diagnosed as HCC by postoperative pathological report, this study has been authorized by the Ethical Review Committee of the First Affiliated Hospital of Guangxi Medical University [Approval Number: 2023-E071-01].

Cell Culture and Transfection

The source of Hep3B and Huh-7 cells was same with previously study,[27] cells were bred with the DMEM medium (Gibco, USA) which contained 10% fetal bovine serum (FBS, Gibco, USA) and 1% streptomycin (Solarbio, China) in an 5% CO2 and 37°C incubator.

A siRNA kit of *PUS1* packaged with siRNA-1, −2, −3 and -negative control (NC) was designed by the Hanbio Biotechnology company (China), and was applied to conduct the cell transfection according to the specification of lipo8000™ transfection reagent (Beyotime, China). We extracted the cells RNA and protein at the 48 and 72 hours after transfection respectively, and performed the PCR and Western blot (WB) to determine the transfection efficiency, the steps of PCR were mentioned previously. The cell proliferation, ROS, migration, and invasion assay were conducted after 48 hours of transfection.

Western Blot Assay

The RIPA reagent (Thermo Fisher Scientific, USA) and the 1% PMSF solution (Thermo Fisher Scientific, USA) were added to derive cells protein, a BCA protein assay kit (Thermo Fisher Scientific, USA) was adopted for measuring protein concentration, then adding 4 times volume of protein loading buffer to it. Because the molecular weight of *PUS1* is close to the *GAPDH*, and could not be cut in an SDS-PAGE gel, therefore two gels were employed to separate protein in same loading quantity and electrophoresis condition. The polyvinylidene difluoride (PVDF) membranes were applied to transferred the protein from the gels, and were closed via 5% skim milk for 1 hour. After that, The PVDF membranes were washed twice and reacted with primary antibody diluent in 4°C overnight. Washing again, and incubating them with secondary antibody diluent at 23°C for 1 hour. The protein bands were displayed with the Bio-Rad ChemiDoc MP Imaging System and analyzed by image J software. The antibodies of *PUS1* and *GAPDH* both were purchased from the Proteintech company.

Cell Proliferation Assay

A Cell Counting Kit-8 (CCK8, Beyotime, China) was adopted to detect the proliferation of siRNA-1 and NC groups in 96-well plate, each group was repeated four times with the same well which containing 100ul of 10% FBS medium and 2000 cells. Five of such 96-well plates were prepared to measure the value of optical density (OD) at 0h, 24h, 48h, 72h, and 96h using Varioskan LUX enzyme labeler (Thermo Fisher Scientific, USA).

ROS Level Comparison

To explore the relation of *PUS1* and ROC production, a ROS Assay Kit (Beyotime, China) was purchased to compare the ROC level between siRNA-1 and NC groups. Each group was repeated three times with same concentration of cell suspension in 96-well plate, after the cells were fully adhered to the bottom of the plate, we diluted the fluorescent probe DCFH-DA to 1:1000 ratio with serum-free DMEM medium and added it to each wells. After 20 minutes, washing twice with DMEM medium and detecting the fluorescence intensity of the cells with the Varioskan LUX enzyme labeler.

Cell Migration and Invasion Assay

The 24-well plate contained the Matrigel (Corning, USA) and the 24-well plate without Matrigel (Corning, USA) were applied for invasion and migration assay respectively. 200ul serum-free suspension with 100,000 cells were put into the upper chamber, and 600ul of 10% FBS DMEM medium was placed into the under chamber. After incubated for 48 hours, the cells were washed twice with PBS, cemented with 4% paraformaldehyde for 30 minutes, and dyed with crystal violet solution for 20 minutes. Non-migrated cells were gently erased off by cotton swabs, and rewashed three times with PBS. The invaded or migrated cells were viewed and pictured under microscope.

Wound-Healing Assay

When the cell density reached 95–100% of 6-well plate after 48 hours of transfection, a straight cell wound was scratched by a 200-μL suction tip. We used PBS to gently wash off the shed cells and added the serum-free medium. After then, the area of wound was sighted and photographed by microscope at 0 h and 24 h.

Statistical Analysis

T-test, Kaplan-Meier analysis, and Cox proportional hazards regression model were achieved by using SPSS 22.0 software, the hazard ratio (HR) and 95% confidence interval (CI) resulted from Kaplan-Meier analysis and Cox proportional hazards regression model were adopted to evaluate the relative risk, $p < 0.05$ was considered statistically significant.

Results

Identifying *PUS1* as the Differential and Prognostic Gene

Through TCGA and ICGC cohorts, we found that *PUS1, PUS7, PUS7L, RPUSD1, RPUSD2 and RPUSD3* significantly were up-regulated in HCC tissues, while *PUS10* was significantly down-regulated (Figure 1A and B). Univariate Cox survival analysis revealed that *PUS1* expression level was observably related to OS in TCGA and ICGC cohorts (Figure 1C and D), which was identical with the results of GEPIA database (Figure 1E–G). In GEPIA, the expression of *PUS7, PUS7L, RPUSD1, RPUSD2* and *RPUSD3* were higher in HCC tissues, on the contrary, we found that *PUS10* had a lower expression in HCC tissues (Figure S1). About the survival analysis, HCC patients with high expression of *PUS7, RPUSD1 and RPUSD3* had a shorter OS compared with low expression (Figure S1), *PUS1* and *PUS7* were found to be correlated with RFS of HCC (Figures 1H, and S1). We found that only the results of *PUS1* were consistent in TCGA, ICCG and GEPIA database, therefore we determined *PUS1* as the differential and prognostic gene for following study.

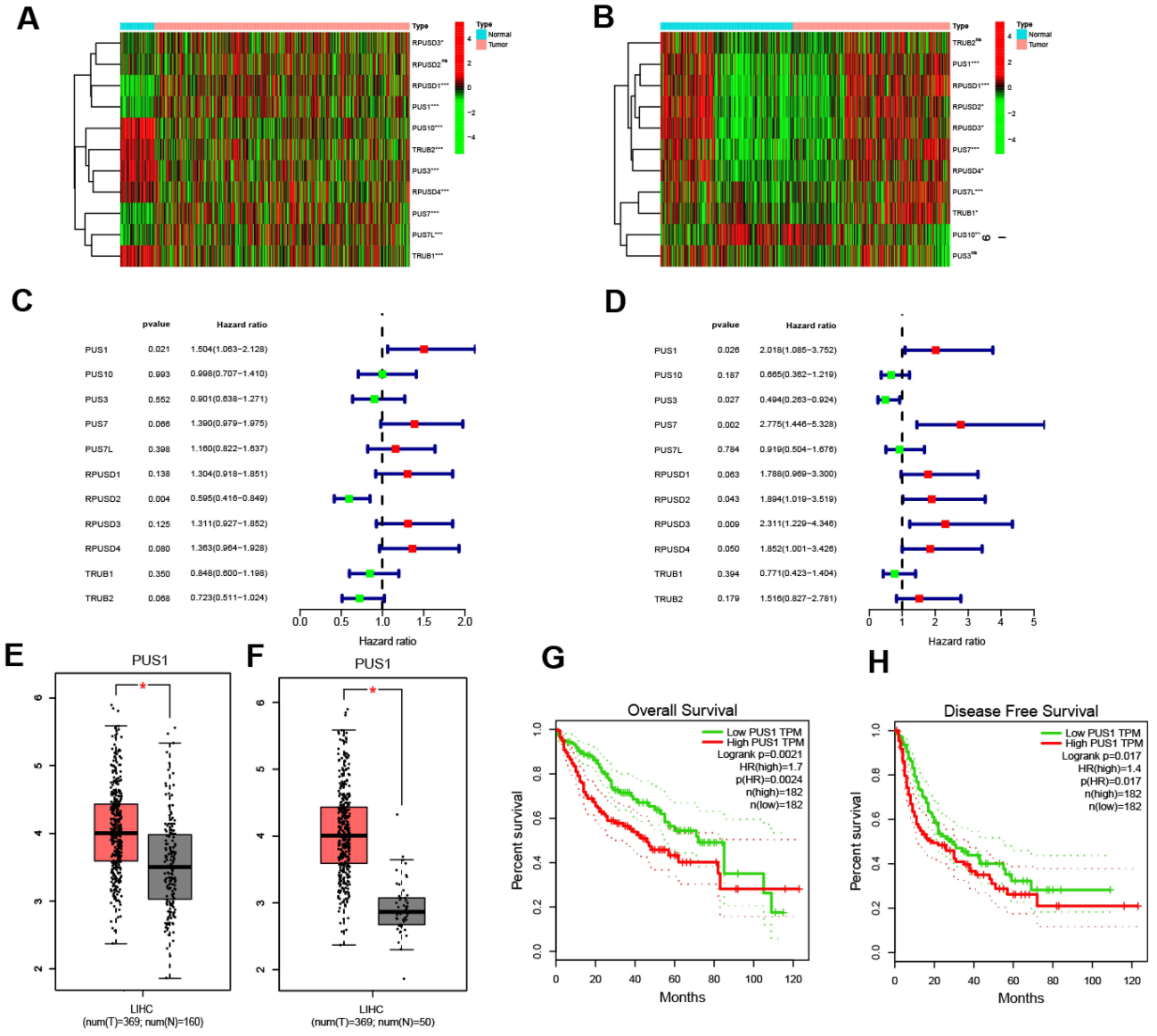

Figure 1 Identification of differential and prognostic genes of PUS enzymes. (**A** and **B**) Heatmap is displayed for the differential expression of PUS enzymes in TCGA and ICGC cohort. (**C** and **D**) Forest plot for univariate cox regression analysis of PUS enzymes in TCGA and ICGC cohort. (**E**) Boxplot of *PUS1* based on TCGA and GTEx data in GEPIA. (**F**) Boxplot of *PUS1* based on TCGA data in GEPIA. (**G** and **H**) Survival plots of *PUS1* for OS and DFS in GEPIA. *p<0.05, **p<0.01, ***p<0.001.
Abbreviation: ns, not significant.

The Clinicopathological Features and Diagnostic Value of *PUS1*

Besides TCGA and ICGC cohorts (Figure 2A and B), we discovered that *PUS1* expression of HCC tissues was also obviously upregulated in GSE14520 cohort (Figure 2C), and PCR results verified the differential expression of *PUS1* (Figure 2D). What's more, the ROC curve indicated that the expression of *PUS1* possessed a value for identifying the HCC and normal liver tissue in these three cohorts (Figure 2E–H). About the correlation between *PUS1* expression with the clinicopathological variables, we found that overexpressed *PUS1* was significantly associated with AFP>300 ng/mL, male, a neoplasm histological grade of G3/G4, and hepatitis B virus (HBV) infection using TCGA cohort (Figure 2I–L), and patients with an advanced stage of TMN or BCLC stage, emerged a higher expression level of *PUS1* in ICGC and GSE14520 cohorts (Figure 2M and O). Noticeably, there was a significant relation between *PUS1* with serum AFP>300 ng/mL in both TCGA and GSE14520 cohorts (Figure 2I and N).

The Prognostic Significance of *PUS1*

The results of K-M analysis of clinicopathological variables and the baseline information of TCGA, and GSE14520 cohort were showed in Tables S1–S4. Univariate and multivariate survival analysis revealed that overexpression of *PUS1* was significantly relevant to a poor OS and was an independent prognostic risk factor to HCC (Figure 3A, B, D, E, G and H). We performed the univariate and multivariate survival analysis about RFS to verify the results of GEPIA using TCGA and GSE14520 cohorts, however *PUS1* was only detected to be significantly correlated with RFS in GSE14520 cohort (Figure 4A). Interestingly, *PUS1* was found to be associated with 1 year-RFS in both GSE14520 and TCGA

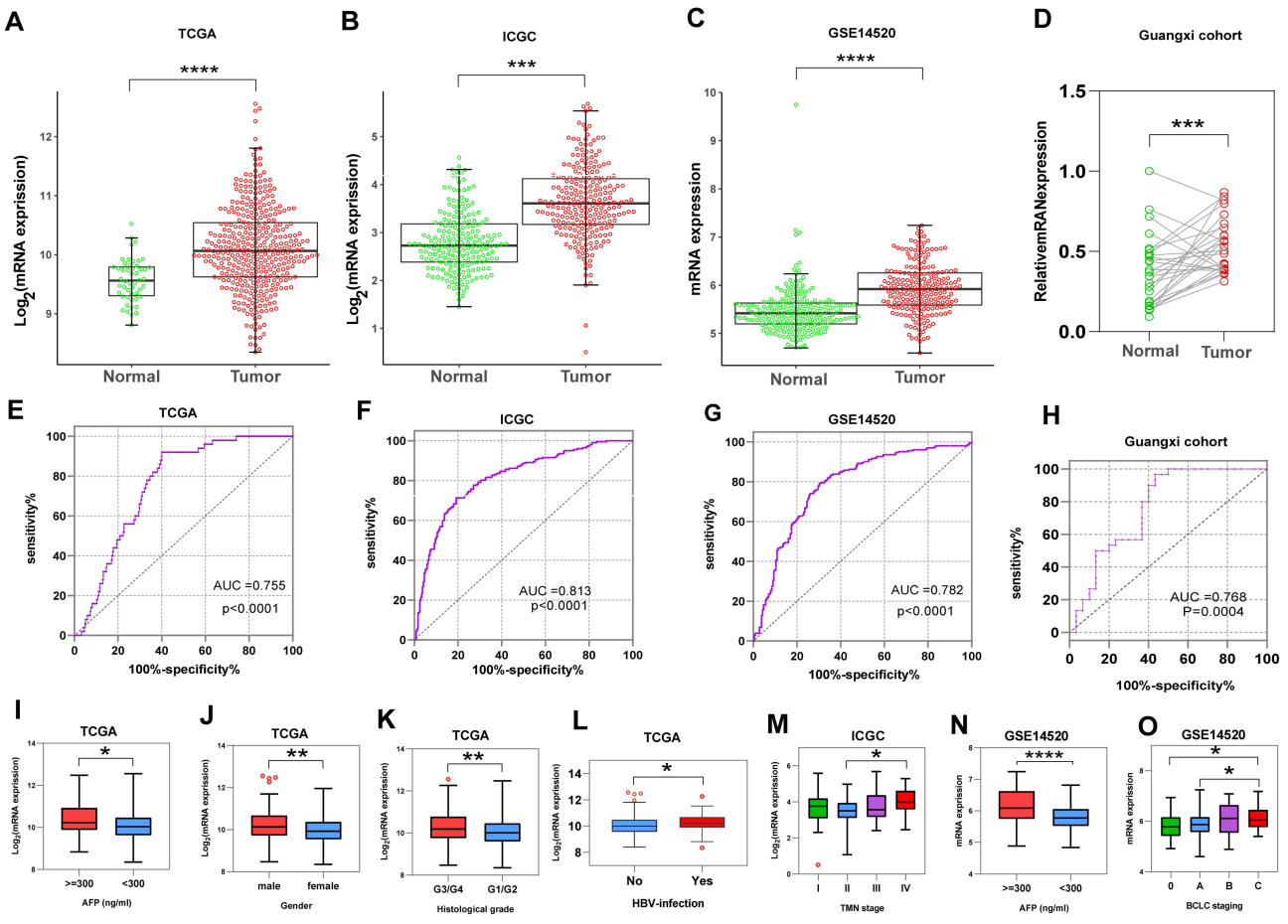

Figure 2 Differential expressions analysis and diagnostic receiver operator curves of *PUS1*. (**A**–**D**) Scatter plots of *PUS1* in TCGA, ICGC, GSE14520 and Guangxi cohorts. (**E**–**H**) Diagnostic receiver operator curves of *PUS1* in TCGA, ICGC, GSE14520 and Guangxi cohorts. (**I**–**O**) Box plot shown the significant clinical characteristics for differential expressions analysis of *PUS1* in TCGA, ICGC and GSE14520 cohorts. *p<0.05, **p<0.01, ***p<0.001, ****p<0.0001.

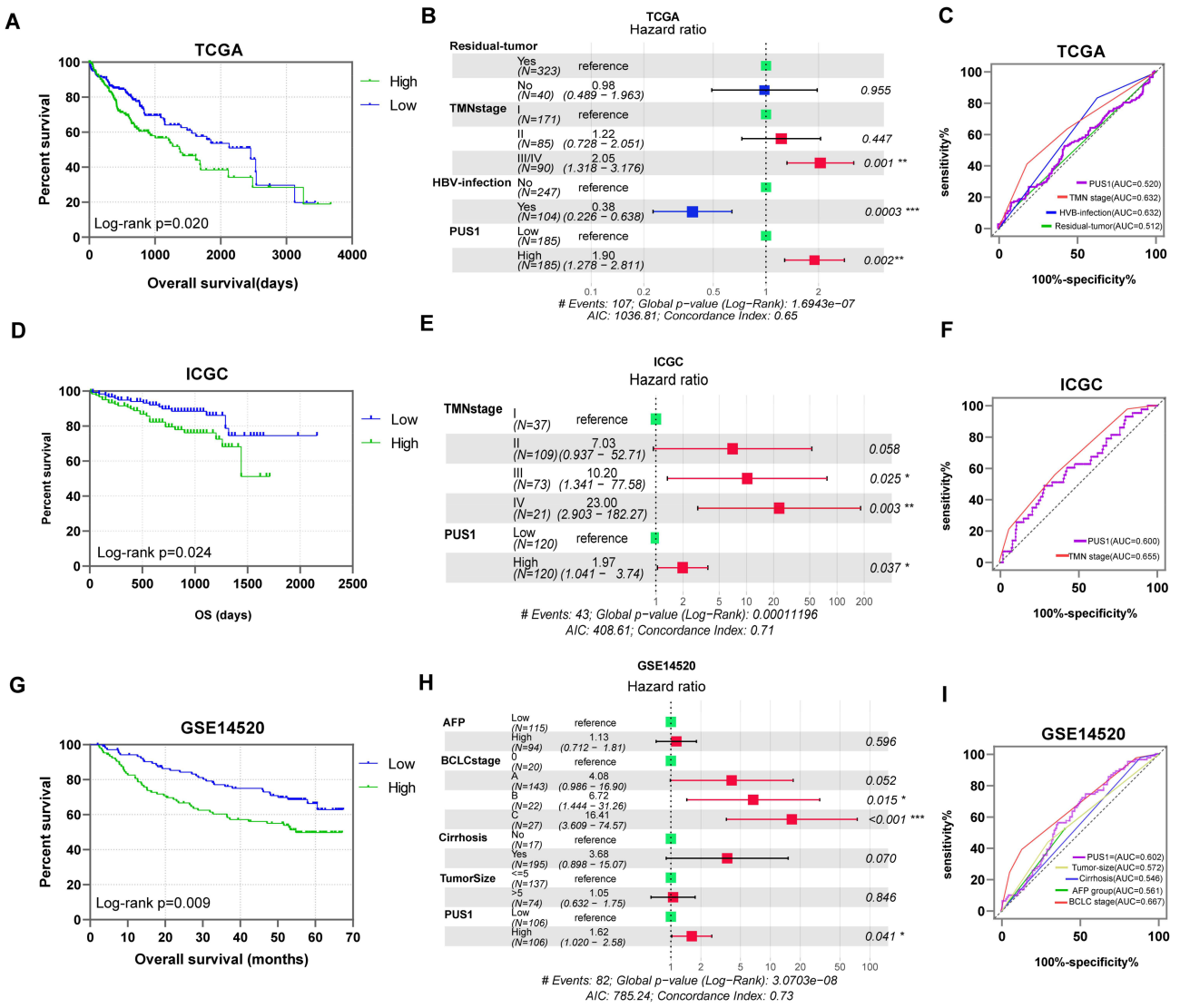

Figure 3 Prognostic OS analysis of *PUS1*. (**A, D** and **G**) Kaplan-Meier plots of *PUS1* in TCGA, ICGC, and GSE14520 cohorts. (**B, E** and **H**) Forest plots for cox proportional hazards regression model of *PUS1* in TCGA, ICGC, and GSE14520 cohorts. (**C, F** and **I**) Prognostic receiver operator curves of *PUS1* and significant clinical characteristics TCGA, ICGC, and GSE14520 cohorts. *p<0.05, **p<0.01, ***p<0.001.

cohorts (Figure 4C and E). Furthermore, the prognostic ROC curve manifested that *PUS1* expression had an efficiency for assessing the OS and 1 year-RFS of HCC (Figures 3I and F and 4D and F). Unfortunately, the performance was not ideal in TCGA cohort (Figure 3C). Joint-effect analysis demonstrated that patients with overexpressed *PUS1* had a poorer outcome when had another risk factor meanwhile (Tables S5–S7). For example, patients combined high *PUS1* expression with a high AFP or a late BCLC stage had a higher risk of death or 1 year-recurrence compared to those conjoined with low AFP level or early BCLC stage in GSE14520 cohort (Figure 5A, C, G and H and Table S5). In TCGA cohort, we found that patients with high *PUS1* expression and TMN stage III/IV had a shorter OS and 1-year RFS than those with low *PUS1* expression and TMN stage I/II (Figure 5D and I).

The Predictive Performance of *PUS1* for Prognosis

The calibration plots disclosed that the nomograms of GSE14520 cohort had good coincidence between predicted and realistic 1-, 3- and 5-year survival rates (Figure 6A), and the 3-year survival rate was coincident in TCGA cohort (Figure S2). The predicted 1-year recurrence rate was observed to be nearly consistent with the reality in GSE14520 and TCGA cohorts (Figure S3). In risk

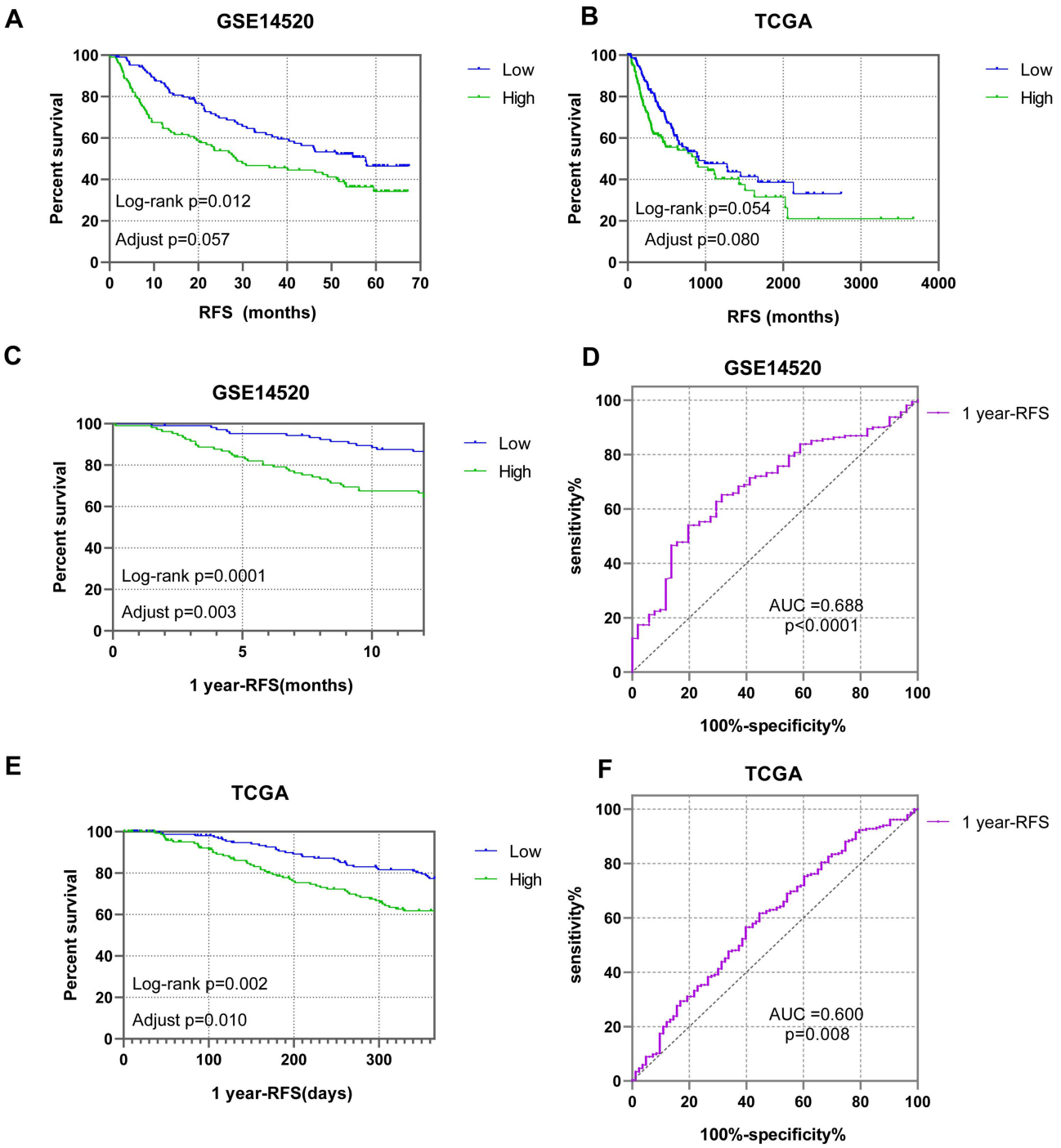

Figure 4 Prognostic RFS analysis of *PUS1*. (**A** and **B**) Kaplan-Meier plots of *PUS1* in TCGA and GSE14520 cohorts. (**D** and **F**) Kaplan-Meier plots and receiver operator curves of *PUS1* for 1 year- RFS in TCGA cohort. (**C** and **E**) Kaplan-Meier plots and receiver operator curves of *PUS1* for 1 year- RFS in GSE14520 cohort.

score models, it was visually displayed that the mortality of HCC increased along with *PUS1* expression, and HCC patients with lower *PUS1* expression lived longer. ROC curves indicated that risk score model performed a well predictive value for the prognosis of HCC at 1-, 2-, 3-, 4-, and 5- years in GSE14520 cohort (Figure 6B). Yet, the risk model of TCGA cohort performed a predictive efficiency for prognosis only at 2- and 3-year with AUC=0.582 (Figure S4).

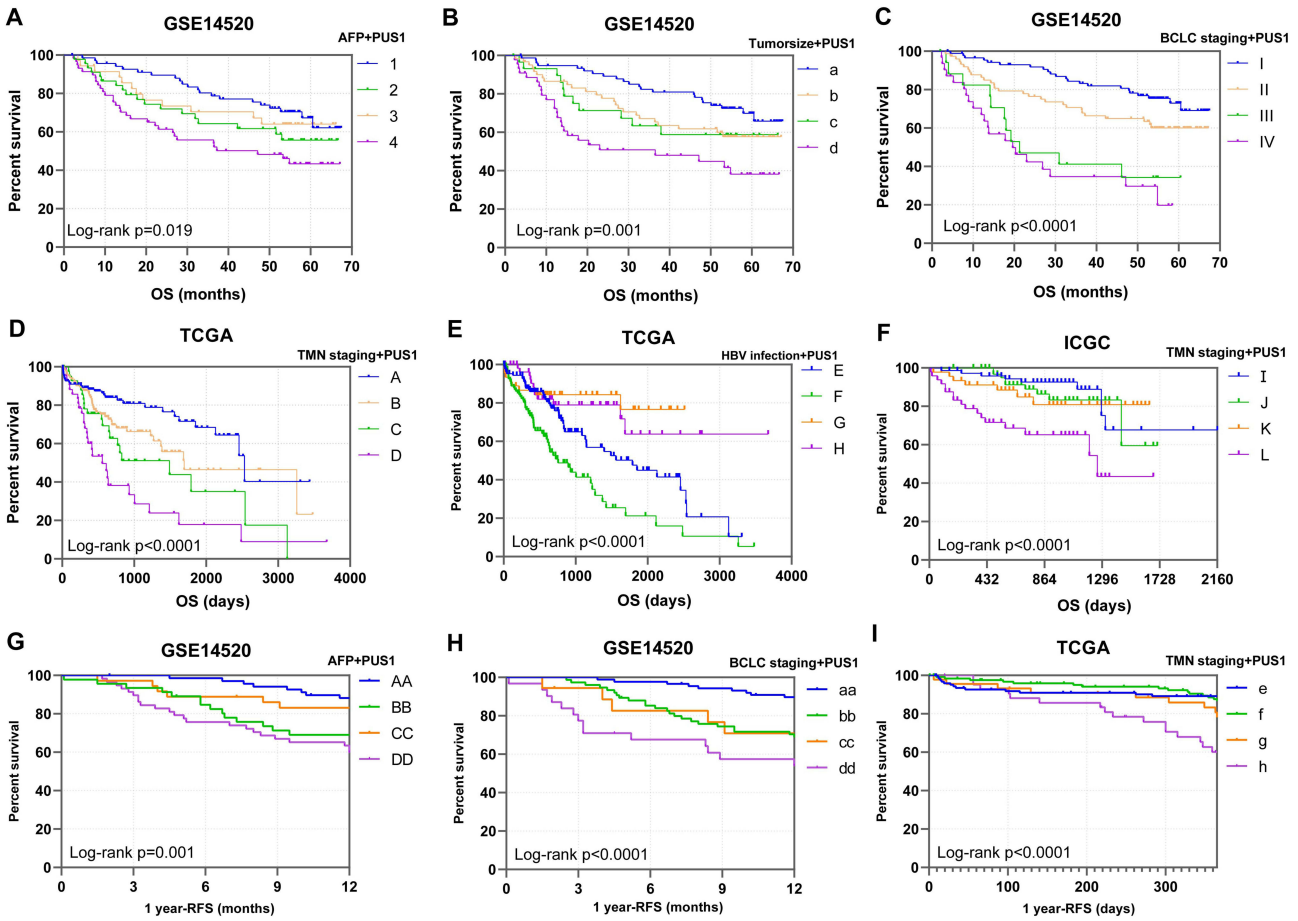

Figure 5 Joint-effect analysis of *PUS1* and significant clinical variables. (**A**–**F**) Kaplan-Meier plots of joint-effect analysis for OS in GSE14520, TCGA and ICGC cohorts. (**G**–**I**) Kaplan-Meier plots of joint-effect analysis for 1 year- RFS in GSE14520 and TCGA cohorts.

Functional Enrichment Analysis

We accomplished the genome-wide correlation analysis of *PUS1*, and the differential analysis to obtain the co-expression genes and differential genes in TCGA and GSE14520 cohorts, the results were listed in Tables S8–S11. Some genes of important pathways were showed with the co-expression network (Figure 7A and B).

Next, through the DAVID analysis of Gene Ontology (GO) and Kyoto Encyclopedia of Genes and Genomes (KEGG) in TCGA and GSE14520 cohorts, it was suggested that *PUS1* and its co-expressed genes may participate in metabolic pathways, oxidative phosphorylation and mitochondrion (Figure 7C and D), the results of differential genes revealed that dysregulated expression of *PUS1* may affected metabolic pathways, bile secretion, drug metabolism, lipid metabolic process, and fatty acid degradation, etc (Figure 7E and F). In TCGA cohort, the GSEA analysis indicated that mitochondrial gene expression, abnormal activity of mitochondrial respiratory chain, oxidative phosphorylation, NF-KB signaling, liver cancer survival down, HIF1a pathway, MYC pathway, apoptosis and NAFLD were enrichment in *PUS1* high-expressed group (Figure 8). And the GSEA analysis using GSE14520 cohort discovered that high *PUS1* expression group may participate in positive regulation of gene expression, cell cycle checkpoint, positive regulation of cell cycle, mitochondrion localization, and regulation of signal transduction, MYC active pathway, P53 regulation pathway, apoptosis, and decreasing the survival of liver cancer (Figure 8).

Knockdown of *PUS1* Restrained the Proliferation, Invasion, Migration and Improve the ROS Level of HCC Cell

The results of PCR and WB showed that si-1 had the best silencing efficiency at both mRNA and protein level (Figure 9). So si-1 was adopted for further experiments.

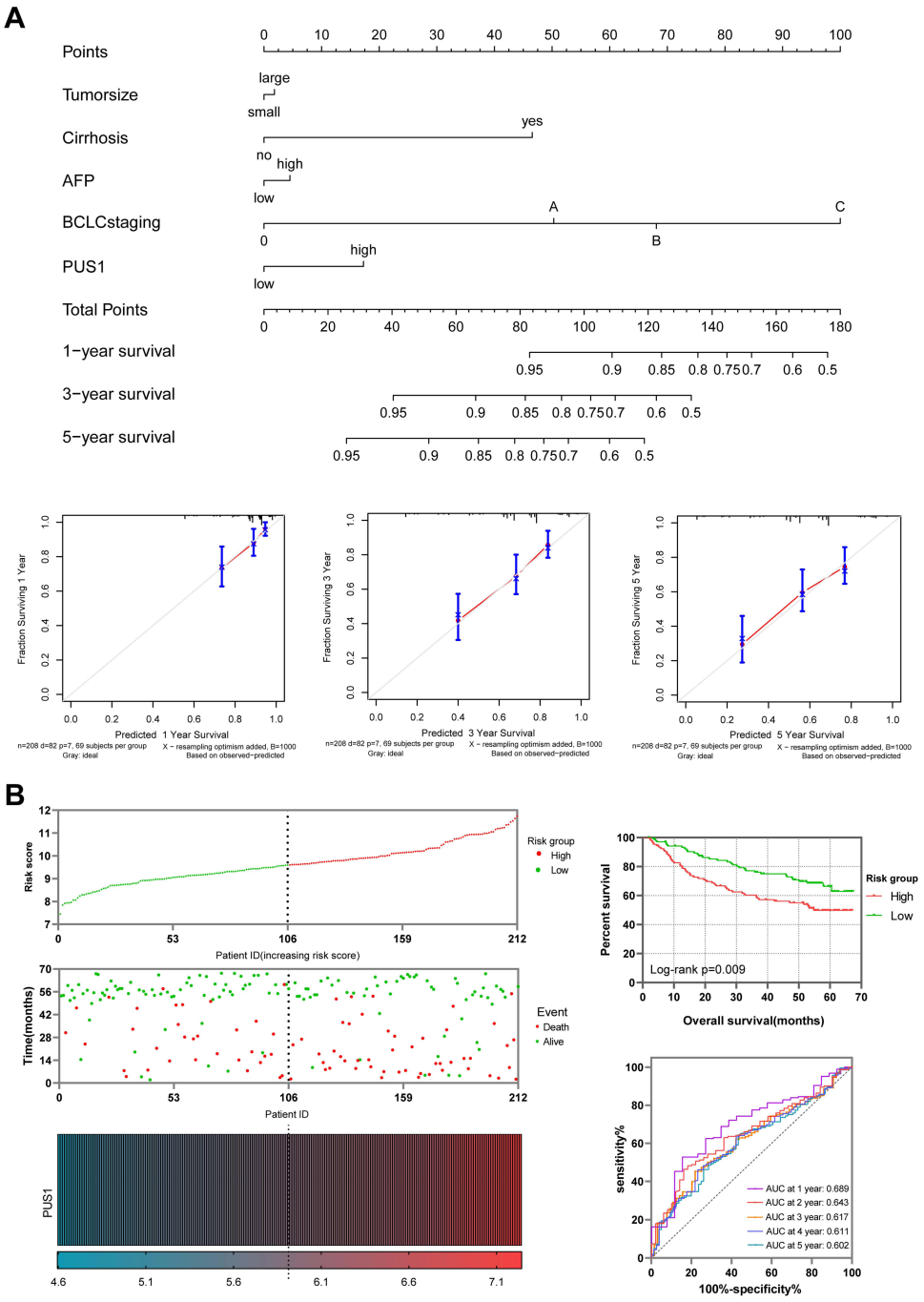

Figure 6 Predictive signature of *PUS1* for prognosis. (**A**) A nomogram of *PUS1* and prognosis related variables for predicting 1-, 3- and 5-year events (death) in GSE14520 cohort. (**B**) A risk model of *PUS1* in GSE14520 cohort.

CCK-8 assay indicated that knockdown of *PUS1* significantly restrained cell proliferation of Hep3B and Huh-7 cells compared with NC group (Figure 10B). ROS assay showed that si-1 group significantly had a higher ROS level than the NC group (Figure 10C). Transwell invasion assay revealed that cells crossed the membranes were significantly less in the si-1 than NC group for both Hep3B and Huh-7 cells, and si-1 group possessed a weaker invasive ability than NC group (Figure 10A). Wound healing assays were used to determine cell migration ability manifested that suppression of *PUS1* significantly reduced the migration ability of Hep3B and Huh-7 cells compared to NC group (Figure 11), this result was consistent with transwell migration assay (Figure 10A).

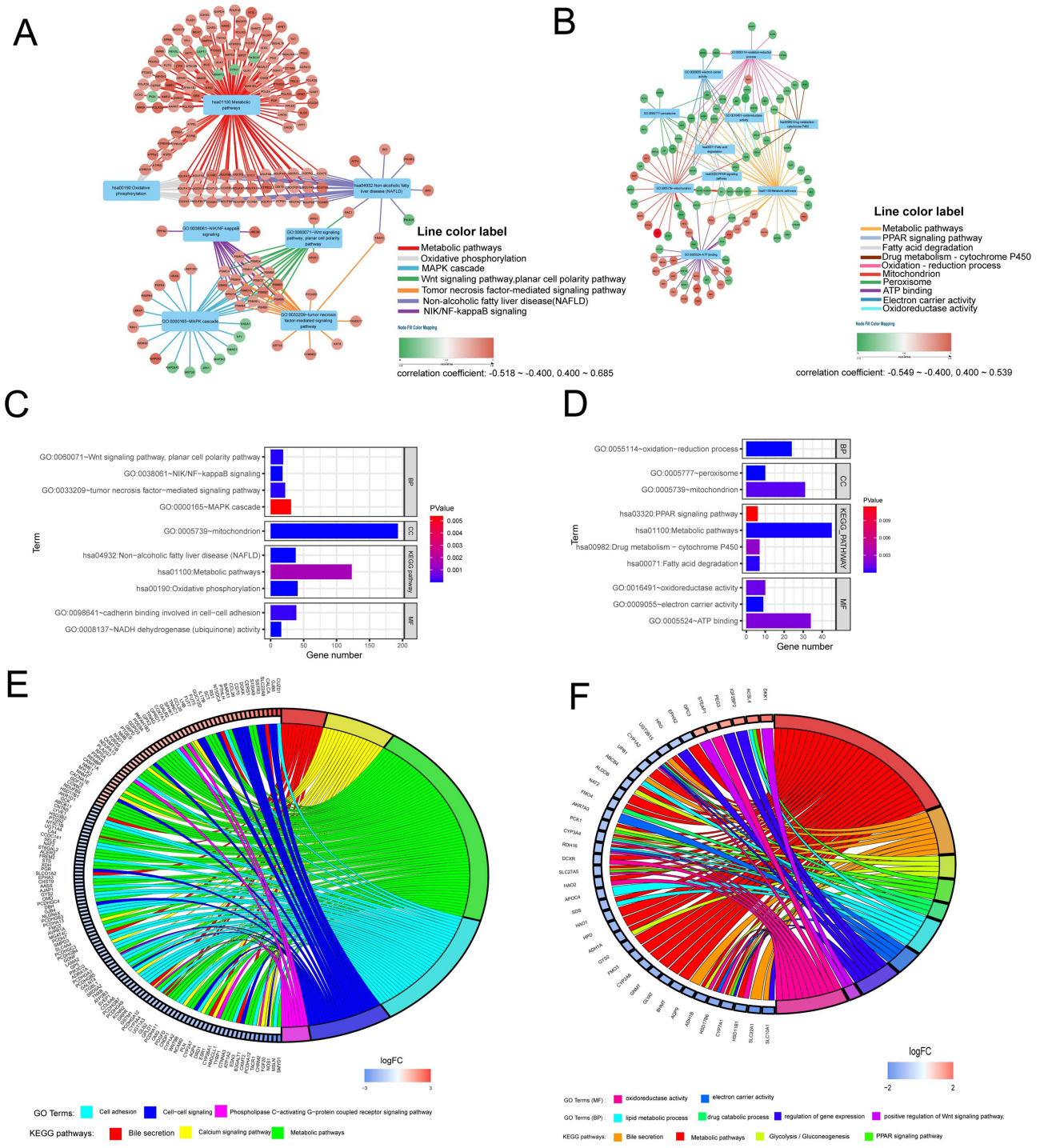

Figure 7 Functional enrichment analysis of *PUS1* co-expression genes and differential genes. (**A** and **B**) Regulatory network of *PUS1* co-expressed genes for several important GO terms and KEGG pathways in TCGA and GSE14520 cohorts. (**C** and **D**) Histogram for functional enrichment analyses of *PUS1* co-expressed genes in DAVID using TCGA and GSE14520 cohorts. (**E** and **F**) Chord plots for functional enrichment analyses of *PUS1* differential genes in DAVID using TCGA and GSE14520 cohorts.

Discussion

In our study, we found that *PUS1* was significantly overexpressed in HCC tissues, and was related to a prognosis of HCC in TCGA, ICCG, GSE14520 and GEPIA. The differential expression of *PUS1* also was validated by Guangxi cohort, ROC curve analysis displayed that expression of *PUS1* had a diagnostic value for HCC. In addition, a higher expression level of *PUS1* was found to be related to some unpromising clinicopathological features such as an advanced BCLC

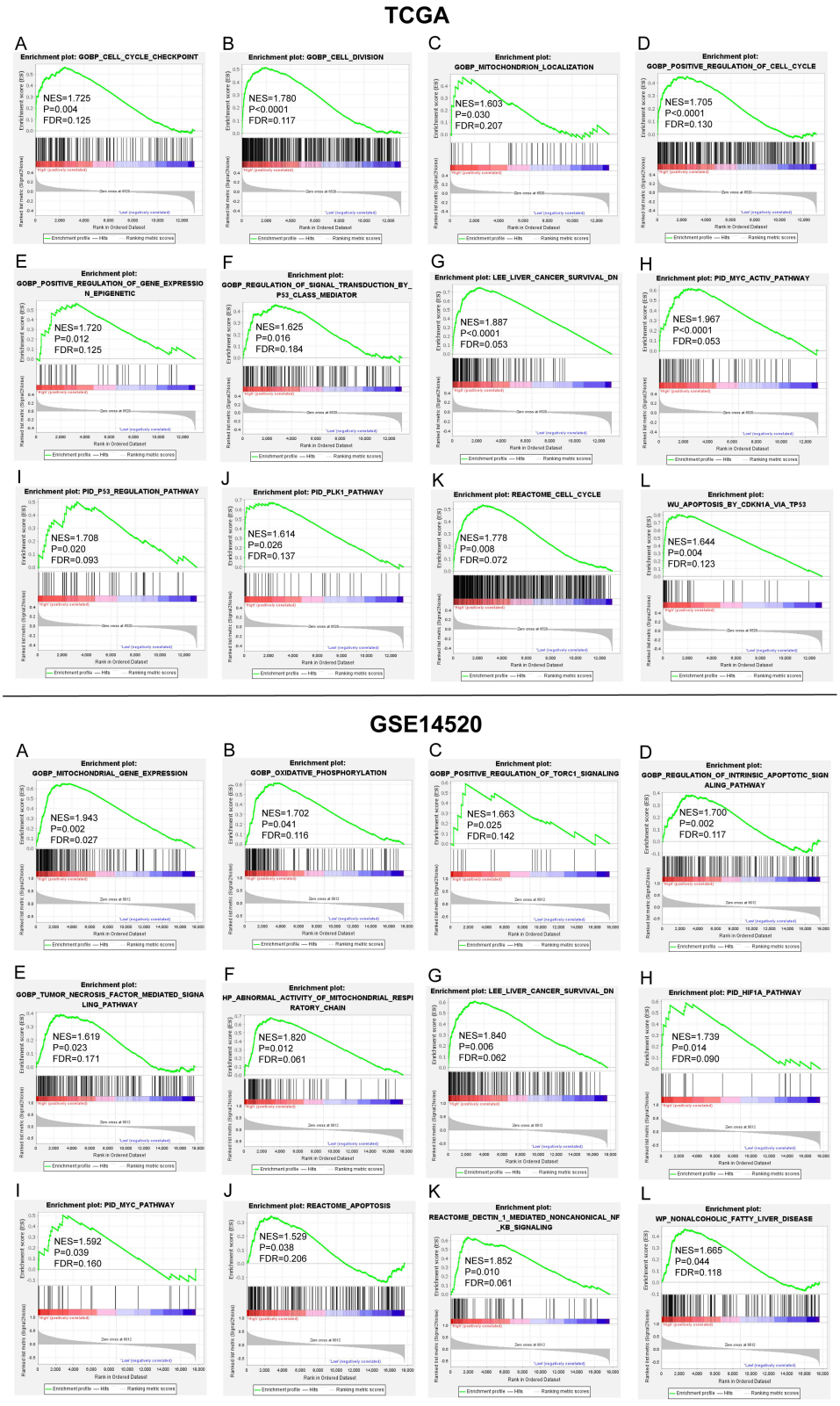

Figure 8 Gene set enrichment analysis of *PUS1* using TCGA data. A, F: Results of c5-reference gene sets for high expression group of *PUS1*. G, L: Results of c2-reference gene sets for high expression group of *PUS1*.

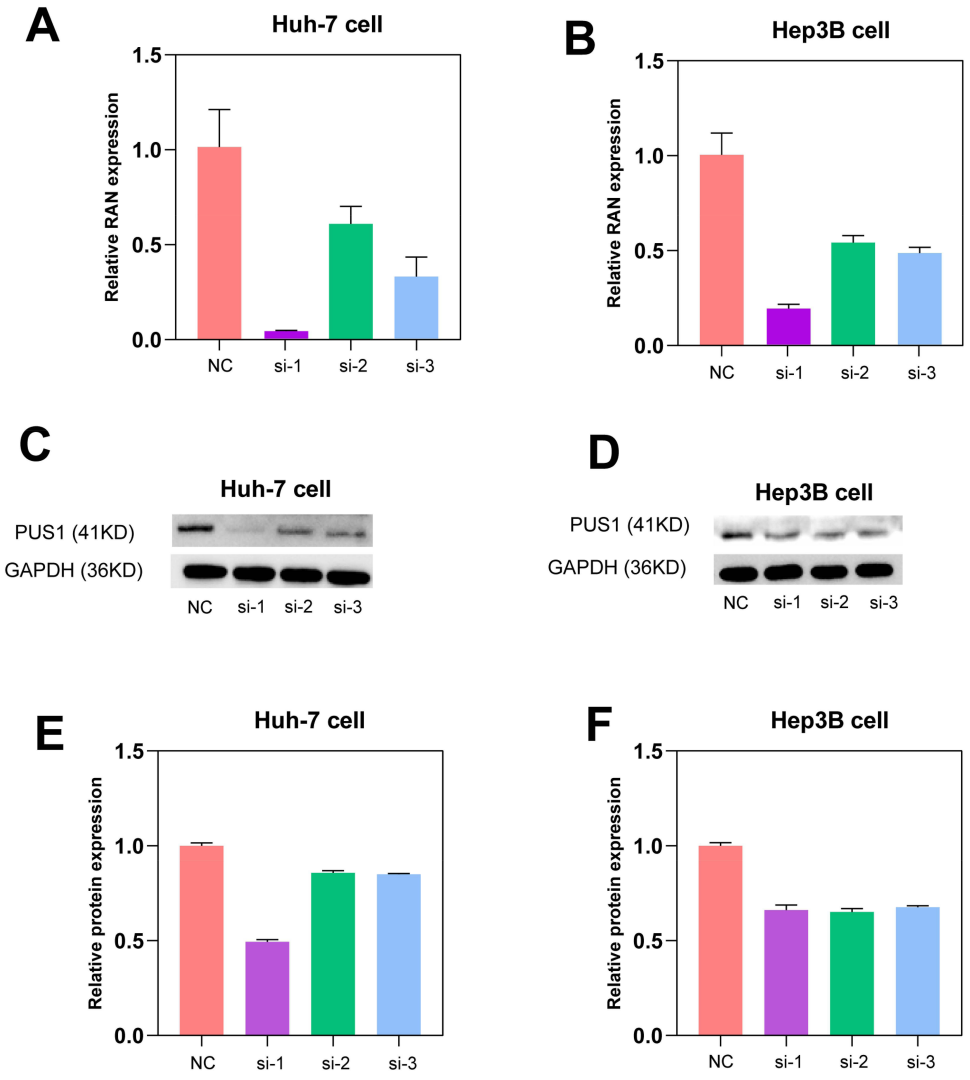

Figure 9 Validation of knockdown efficiency of *PUS1*. (**A** and **B**) Results of PCR after knock-downing *PUS1* in Huh-7 and Hep3B cells. (**C** and **D**) Results of WB after knock-downing *PUS1* in Huh-7 and Hep3B cells. (**E** and **F**) Histogram displaying the results of WB.

stage, TNM stage, or a higher serum AFP level. The Cox proportional hazards regression model showed that *PUS1* was an autocephalous risk factor for HCC. It was worth mentioning that *PUS1* was detected to be significantly connected with the RFS in GEPIA and GSE14520 cohort, but it was not statistically significant with a *p* value greater than but close to 0.05 in TCGA cohort. We speculated that the samples may be not insufficient, and the connection of *PUS1* and RFS remains to be further explored in future. Interestingly, we noticed that high *PUS1* expression was concerned with a poor 1 year-RFS in GSE14520 and TCGA cohorts. ROC analysis manifested that *PUS1* possessed a certain value on assessing the OS and 1-year-RFS for HCC, it was a pity that the area under of ROC curve was not ideal in TCGA cohort. Similarly, the nomogram indicated that the predicted survival rate of *PUS1* was basically consistent with the practical survival rate in the GSE14520 cohort, and the risk score model possessed a good prognostic efficiency for 1-, 2-, 3-, 4- and 5-year OS of HCC in the GSE14520 cohort, but it has not performed satisfactory in the TCGA cohort. We detected that *PUS1* expression of HBV-infected patients was higher than those non-HBV-infected patients in TCGA cohort. However, there were small proportion of HBV infection patients in the TCGA cohort, the majority of cases had HBV infection in GSE14520 and ICCG cohorts. We speculated that it may be related to the differences in etiology, and *PUS1* may be more suitable for estimating the prognosis of HBV infected patients in HCC. According to the above results, we concluded that *PUS1* may be a underlying diagnostic and prognostic gene for HCC, which was consistent with the result of Shi' study.[23]

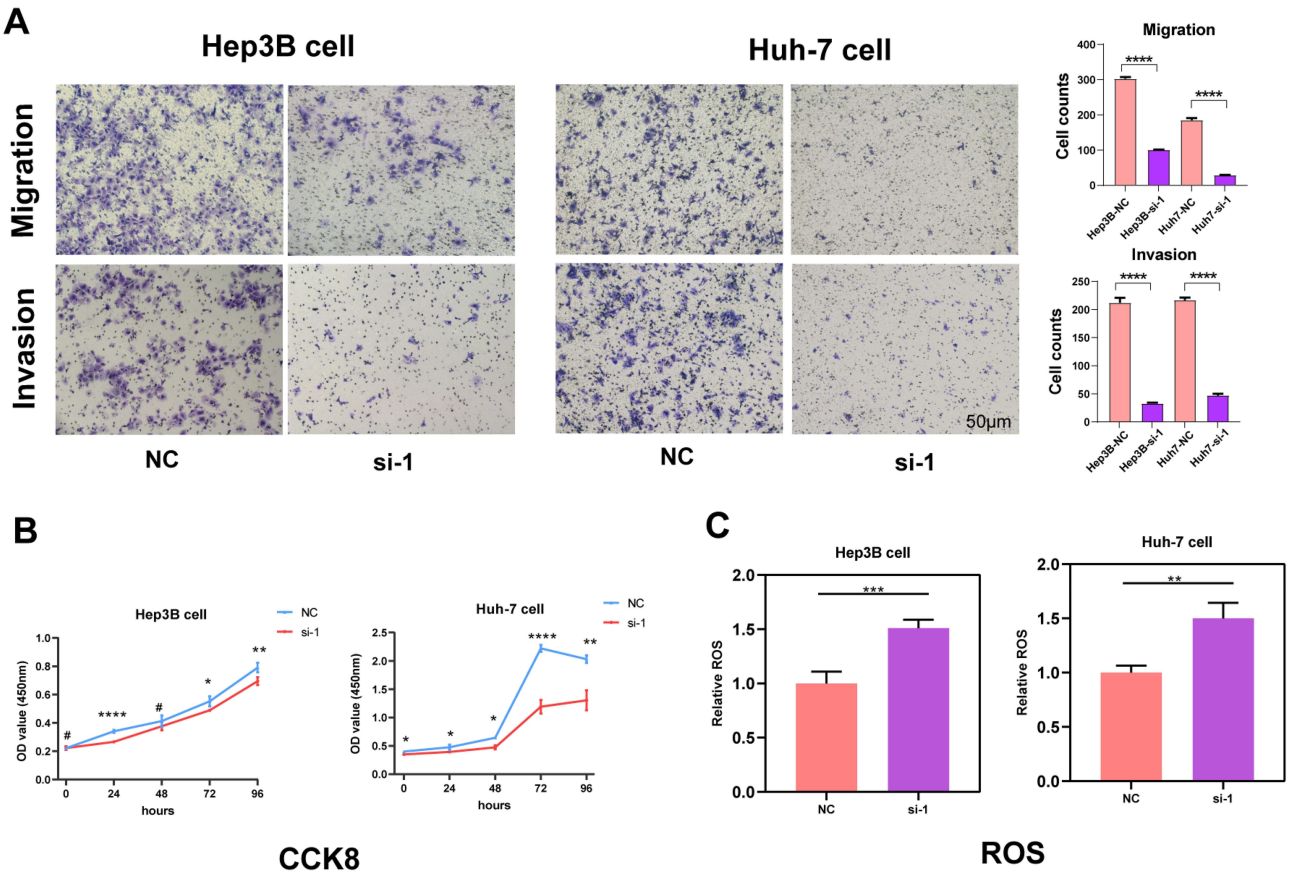

Figure 10 Results of cell migration, invasion, proliferation and ROS level assays. (**A**) Images under microscope and statistical comparison of transwell migration and invasion assays in Hep3B and Huh-7 cells. (**B**) Results of cell proliferation assays of Hep3B and Huh-7 cells. (**C**) Histogram comparing ROS level of NC and si-1 group in Hep3B and Huh-7 cells. *p<0.05, **p<0.01, ***p<0.001, #Not significant.

We also explored the clinical application of *PUS1* by joint-effect analysis, and the result manifested that patients with high *PUS1* expression had a poorer prognosis when had another risk factor.

At present, the research of *PUS1* is still in the stage of eukaryotic microbial. *PUS1* can modify multiple tRNA sites,[28,29] and also involved in mRNA pseudouridylation.[30] The deficiency of *PUS1* was considered to be linked to mitochondrial diseases in human.[18] *PUS1* was found to regulate gene expression through alternative pre-mRNA processing in human,[31] Zhao et al found that *PUS1* enhanced the gene expression of the corresponding nuclear receptor pathways in breast cancer and melanoma cell lines.[32] These researched implied that *PUS1* might impact on the transcriptome. However, there are few literatures to probe the carcinogenesis of *PUS1*, and its mechanism still keeps unclear in HCC.

Genes are often coordinated to perform cellular activities and biological functions,[33] genes which show a trend of simultaneous up-regulation or down-regulation can be identified by co-expression analysis in a group of samples, and this is also a method for inferring the function of target gene and the gene-disease associations from genome-wide genes expression.[34] Therefore, we identified the co-expressed genes and differential genes of *PUS1*, and conducted the enrichment analysis through DAVID to explore the potential functional mechanism of *PUS1*. The results implied that *PUS1* and its co-expressed genes were involved in metabolic pathways, mitochondrial function, oxidative phosphorylation and NADH dehydrogenase activity, etc. The missense mutations of *PUS1* have been reported to defect the mitochondrial pseudouridylation and make abnormal oxidative phosphorylation which caused the mitochondrial myopathy and sideroblastic anemia in humans,[18] this implied that *PUS1* plays a vital role in mitochondrial function and oxidative phosphorylation. Mitochondria are abundant in the liver,[35] its main functions include regulating cell respiration, oxidative phosphorylation, cell death, maintaining the balance of reactive oxygen species (ROS), which participated in

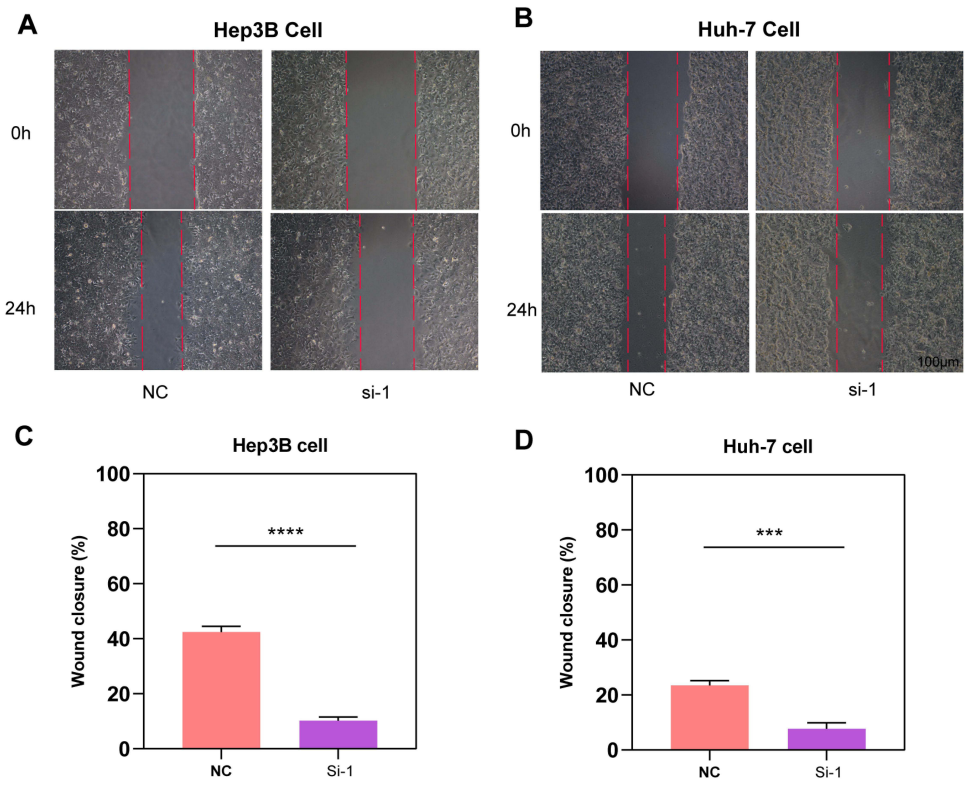

Figure 11 Results of wound-healing assays. (**A** and **B**) Results of wound-healing assays of Hep3B and Huh-7 cells under microscope. (**C** and **D**) Histogram comparing the results of wound-healing assays. ***p<0.001, ****p<0.0001.

energy metabolism and cell homeostasis.[36] Previous studies have shown that mitochondrial dysfunction and mitochondrial stress response were closely related to the cell growth and metastasis of HCC through increasing ROS production and metabolic reprogramming of damaged hepatocytes.[37,38] In our study, the ROS assay have showed that down-regulation of *PUS1* improved the ROS level of HCC cells, this only suggested that *PUS1* is associated with ROS production, because different concentrations of ROS can contribute to the development of cancer, also can trigger cell death to promote cancer treatment.[39] In addition, *PUS1* was found to be overexpressed in tumor tissues and cause poor outcomes in breast cancer. These literatures provided some supports that up-regulation of *PUS1* may play a carcinogenic role on HCC by involving in mitochondrial function, oxidative phosphorylation, ROS production and metabolic pathways.

Interestingly, the DAVID and GSEA analysis using TCGA cohort demonstrated that the gene set, NAFLD, was enrichment in co-expressed genes of *PUS1* and high *PUS1* expression group. Furthermore, enrichment analysis indicated that the differential genes of *PUS1* expression group were involved in some biological processes and pathways which have been verified to take part in the pathogenesis of non-alcoholic steatohepatitis (NASH) related HCC in mouse models,[40] such as metabolic pathways, calcium signaling pathway, bile secretion and cell adhesion. NAFLD is one of the dangerous factor of HCC, and NASH is the inflammatory stage of NAFLD, which can progress to cirrhosis and HCC.[41] At present, what regarding the mechanism of NAFLD progression to NASH, the classical two-hit theory thought that hepatic steatosis triggered oxidative stress which centered on mitochondrial reactive oxygen species and then leads to lipid peroxidation, release of inflammatory molecules, mitochondrial damage, and further damage to the liver.[42] The novel "multiple hit theory" argued that NASH was a interaction of genetic variation, abnormal lipid metabolism, oxidative stress, mitochondrial dysfunction, release of inflammatory cytokines and adipokines, bile acids, and imbalance of the gut microbiota, etc.[43] Combining with above functional analysis and reported literature, *PUS1* seems to be correlated with NAFLD-related HCC through metabolic pathways, oxidative phosphorylation and mitochondrial

function. However, our study has insufficient NAFLD-related HCC cases, the relation between overexpression of *PUS1* and NAFLD-related HCC remains to be further explored.

Moreover, functional enrichment analysis disclosed that *PUS1* may work in the development of HCC by participating in several important cancer pathways. For example, it was suggested that *PUS1* may implicate in NIK/NF-kappaB signaling, WNT signaling pathway, MAPK cascade, tumor necrosis factor-mediated signaling and MYC pathway in TCGA cohort. The activation of MAPK and WNT signaling pathway can promote the cell proliferation, growth and angiogenesis of HCC.[44] Tumor necrosis factor-mediated signaling and NIK/NF-kappaB signaling pathways promote the pathogenesis of HCC by regulating hepatic inflammation and immune response.[45,46] Available studies have shown that c-MYC drove HCC development in mice by involving in multiple signals.[47–49] GSE14520 cohort showed that *PUS1* may be related to apoptosis, positive regulation of cell cycle, MYC pathway, positive regulation of gene expression, PLK1 pathway and P53 pathway. P53 was considered to be a transcription factor that promotes or blocks the target genes to impact on cell cycle, apoptosis, programmed necrosis, angiogenesis and immune regulation, it involved in the pathogenesis and progression of many types of cancer.[50] These results hinted that *PUS1* may affect the cell phenotypes of HCC. In addition, *DKC1* and *PUS7*, which have a co-expression relationship and certain same functions with *PUS1*, had been proved to may be therapeutic target for colorectal cancer by some gene knockdown experiment.[51,52] Therefore, we verified *PUS1* by vitro cell assay, and the results showed that knockdown of *PUS1* significantly weakened the ability of cell proliferation, invasion and migration.

This study firstly proved that down-regulation of *PUS1* can depress the proliferation, invasion, and migration of HCC cells, and increase intracellular ROS levels, which provided the possibility for *PUS1* to treat HCC. However, there are several disadvantages and inadequacies in this study. First, the samples and data are mainly from public databases, the clinical significance of *PUS1* needs to be validated by more cohorts or a strict prospective cohort study. Secondly, the results of functional enrichment analysis lacks of more evidence to support, whether *PUS1* involved in the cancer pathways described previously needs to further validated. Third, this study lacked experiments to verify whether *PUS1* affected cell cycle and apoptosis of HCC cells. Last but not least, in vitro cell experiments lacked an over-expressed group of *PUS1*, and in vivo functional experiments such as animal tumorigenesis model need to be performed to explore the molecular mechanisms of *PUS1*.

Conclusions

In the study, it was demonstrated that *PUS1* was overexpressed in HCC tissues, and was associated with OS and 1 year-RFS for HCC. ROC curves and risk score model manifested that *PUS1* may serve as a diagnostic and prognostic biomarker for HCC. Joint-effect analysis and nomogram highlighted that high expression of *PUS1* as a risk factor for poor prognosis of HCC. Functional enrichment analysis suggested that *PUS1* may be involved in metabolic pathways, mitochondrial function, oxidative phosphorylation, NAFLD and several important cancer pathways. In vitro cell assay revealed that knockdown of *PUS1* significantly inhibits the proliferation, invasion, migration and improved the ROS level of HCC cells. Nonetheless, these many results require further research to validate.

Abbreviations

PUS, pseudouridine synthase; TCGA, The Cancer Genome Atlas; ICGC, International Cancer Genome Consortium; HCC, hepatocellular carcinoma; MST, median survival time; RFS, recurrence-free survival; OS, overall survival; HR, hazard ratio; CI, confidence interval; AFP, alpha fetoprotein; PIVKA-II, Protein Induced by Vitamin K Absence or antagonist-II; GALAD, gender, age, AFP-L3, AFP and des-carboxy-prothrombin; HBV, hepatitis B virus; HCV, hepatitis C virus; GEPIA, Gene Expression Profiling Interactive Analysis; ROC, receiver operating characteristic; DAVID, Database for Annotation, Visualization and Integrated Discovery; GO, gene ontology; KEGG, Kyoto Encyclopedia of Genes and Genomes; GSEA, Gene Set Enrichment Analysis; PCR, polymerase chain reaction; WB, Western blot; ROS, reactive oxygen species; NAFLD, non-alcoholic fatty liver disease.

Data Sharing Statement

The data used to support the findings of this study are included within the article and the Supplementary Information Files.

Ethics Approval and Informed Consent

This study has been authorized by the Ethical Review Committee of the First Affiliated Hospital of Guangxi Medical University [Approval Number: 2023-E071-01]. Written informed consent was agreed and signed by all HCC patients. This study complies with the Declaration of Helsinki.

Acknowledgments

The authors thank the contributors of TCGA, ICGC and GSE14520 database for sharing the HCC dataset on open access. We greatly acknowledge the support of the National Key Clinical Specialty Programs (General Surgery and Oncology) and the Key Laboratory of Early Prevention & Treatment for Regional High-Incidence-Tumor (Guangxi Medical University), Ministry of Education, China. We sincerely appreciate the helpful comments on this study received from editor and reviewers. We are grateful to Zaida Huang, Department of Hepatobiliary Surgery, The First Affiliated Hospital of Guangxi Medical University, Nanning, Guangxi Zhuang Autonomous Region, People's Republic of China, for his help with data collection, data analysis, technical assistance, formatting-related writing assistance in this paper.

Author Contributions

All authors contributed to data analysis, drafting or revising the article, have agreed on the journal to which the article will be submitted, gave final approval of the version to be published, and agree to be accountable for all aspects of the work.

Funding

Innovation Project of Guangxi Graduate Education (YCSW2022227, 02603222064X); Guangdong High-level Hospital Construction Fund (No. ynkt2021-zz07); Guangdong High-level Hospital Construction Fund; Shenzhen High-level Hospital Construction Fund; Key Laboratory of High-Incidence-Tumor Prevention & Treatment (Guangxi Medical University), Ministry of Education (grant nos. GKE2018-01, GKE2019-11 and GKE-ZZ202009); Natural Science Foundation of Shenzhen Science and Technology Innovation Commission (No. JCYJ20220530155610023); Guangxi Key Laboratory for the Prevention and Control of Viral Hepatitis (No. GXCDCKL201902).

Disclosure

The authors report no conflicts of interest in this work.

References

1. Bray F, Ferlay J, Soerjomataram I, Siegel RL, Torre LA, Jemal A. Global cancer statistics 2018: GLOBOCAN estimates of incidence and mortality worldwide for 36 cancers in 185 countries. *CA Cancer J Clin*. 2018;68(6):394–424. doi:10.3322/caac.21492
2. Yang JD, Hainaut P, Gores GJ, Amadou A, Plymoth A, Roberts LR. A global view of hepatocellular carcinoma: trends, risk, prevention and management. *Nat Rev Gastroenterol Hepatol*. 2019;16(10):589–604. doi:10.1038/s41575-019-0186-y
3. Tzartzeva K, Obi J, Rich NE, et al. Surveillance imaging and alpha fetoprotein for early detection of hepatocellular carcinoma in patients with cirrhosis: a meta-analysis. *Gastroenterology*. 2018;154(6):1706–1718 e1701. doi:10.1053/j.gastro.2018.01.064
4. Chen H, Zhang Y, Li S, et al. Direct comparison of five serum biomarkers in early diagnosis of hepatocellular carcinoma. *Cancer Manag Res*. 2018;10:1947–1958. doi:10.2147/CMAR.S167036
5. Yi X, Yu S, Bao Y. Alpha-fetoprotein-L3 in hepatocellular carcinoma: a meta-analysis. *Clin Chim Acta*. 2013;425:212–220. doi:10.1016/j.cca.2013.08.005
6. Yang JD, Addissie BD, Mara KC, et al. GALAD score for hepatocellular carcinoma detection in comparison with liver ultrasound and proposal of GALADUS score. *Cancer Epidemiol Biomarkers Prev*. 2019;28(3):531–538. doi:10.1158/1055-9965.EPI-18-0281
7. Wang W, Wei C. Advances in the early diagnosis of hepatocellular carcinoma. *Genes Dis*. 2020;7(3):308–319. doi:10.1016/j.gendis.2020.01.014
8. Barbieri I, Kouzarides T. Role of RNA modifications in cancer. *Nat Rev Cancer*. 2020;20(6):303–322. doi:10.1038/s41568-020-0253-2
9. He L, Li H, Wu A, Peng Y, Shu G, Yin G. Functions of N6-methyladenosine and its role in cancer. *Mol Cancer*. 2019;18(1):176. doi:10.1186/s12943-019-1109-9
10. Penzo M, Guerrieri AN, Zacchini F, Trere D, Montanaro L. RNA Pseudouridylation in physiology and medicine: for better and for worse. *Genes*. 2017;8(11):11. doi:10.3390/genes8110301
11. De Zoysa MD, Yu YT. Posttranscriptional RNA Pseudouridylation. *Enzymes*. 2017;41:151–167.
12. Terns M, Terns R. Noncoding RNAs of the H/ACA family. *Cold Spring Harb Symp Quant Biol*. 2006;71:395–405. doi:10.1101/sqb.2006.71.034
13. Balogh E, Chandler JC, Varga M, et al. Pseudouridylation defect due to DKC1 and NOP10 mutations causes nephrotic syndrome with cataracts, hearing impairment, and enterocolitis. *Proc Natl Acad Sci U S A*. 2020;117(26):15137–15147. doi:10.1073/pnas.2002328117

14. Dos Santos PC, Panero J, Stanganelli C, et al. Dysregulation of H/ACA ribonucleoprotein components in chronic lymphocytic leukemia. *PLoS One*. 2017;12(6):e0179883. doi:10.1371/journal.pone.0179883
15. Kim MS, Kim SS, Yoo NJ, Lee SH. Expressional analysis of NOLA1, NOLA2, NOLA3 and DKC1, the core proteins in H/ACA riboproteins, in gastric and colorectal cancers. *Pathology*. 2012;44(6):576–577. doi:10.1097/PAT.0b013e3283583bf6
16. Zhang M, Zhao W, Liu S, et al. H/ACA snoRNP gene family as diagnostic and prognostic biomarkers for hepatocellular carcinoma. *Pharmgenomics Pers Med*. 2021;14:1331–1345. doi:10.2147/PGPM.S333838
17. Rintala-Dempsey AC, Kothe U. Eukaryotic stand-alone pseudouridine synthases - RNA modifying enzymes and emerging regulators of gene expression? *RNA Biol*. 2017;14(9):1185–1196. doi:10.1080/15476286.2016.1276150
18. Bykhovskaya Y, Casas K, Mengesha E, Inbal A, Fischel-Ghodsian N. Missense mutation in pseudouridine synthase 1 (PUS1) causes mitochondrial myopathy and sideroblastic anemia (MLASA). *Am J Hum Genet*. 2004;74(6):1303–1308. doi:10.1086/421530
19. de Brouwer APM, Abou Jamra R, Kortel N, et al. Variants in PUS7 cause intellectual disability with speech delay, microcephaly, short stature, and aggressive behavior. *Am J Hum Genet*. 2018;103(6):1045–1052. doi:10.1016/j.ajhg.2018.10.026
20. Jana S, Hsieh AC, Gupta R. Reciprocal amplification of caspase-3 activity by nuclear export of a putative human RNA-modifying protein, PUS10 during TRAIL-induced apoptosis. *Cell Death Dis*. 2017;8(10):e3093. doi:10.1038/cddis.2017.476
21. Zhang Q, Fei S, Zhao Y, et al. PUS7 promotes the proliferation of colorectal cancer cells by directly stabilizing SIRT1 to activate the Wnt/beta-catenin pathway. *Mol Carcinog*. 2023;62(2):160–173. doi:10.1002/mc.23473
22. Du J, Gong A, Zhao X, Wang G. Pseudouridylate synthase 7 promotes cell proliferation and invasion in colon cancer through activating PI3K/AKT/mTOR signaling pathway. *Dig Dis Sci*. 2022;67(4):1260–1270. doi:10.1007/s10620-021-06936-0
23. Jin Z, Song M, Wang J, et al. Integrative multiomics evaluation reveals the importance of pseudouridine synthases in hepatocellular carcinoma. *Front Genet*. 2022;13:944681. doi:10.3389/fgene.2022.944681
24. Fujimoto A, Furuta M, Totoki Y, et al. Whole-genome mutational landscape and characterization of noncoding and structural mutations in liver cancer. *Nat Genet*. 2016;48(5):500–509. doi:10.1038/ng.3547
25. Roessler S, Jia HL, Budhu A, et al. A unique metastasis gene signature enables prediction of tumor relapse in early-stage hepatocellular carcinoma patients. *Cancer Res*. 2010;70(24):10202–10212. doi:10.1158/0008-5472.CAN-10-2607
26. Lin Z, Xu Q, Miao D, Yu F. An inflammatory response-related gene signature can impact the immune status and predict the prognosis of hepatocellular carcinoma. *Front Oncol*. 2021;11:644416. doi:10.3389/fonc.2021.644416
27. Mo S, Fang D, Zhao S, et al. Down regulated oncogene KIF2C inhibits growth, invasion, and metastasis of hepatocellular carcinoma through the Ras/MAPK signaling pathway and epithelial-to-mesenchymal transition. *Ann Transl Med*. 2022;10(3):151. doi:10.21037/atm-21-6240
28. Motorin Y, Keith G, Simon C, et al. The yeast tRNA: pseudouridine synthase Pus1p displays a multisite substrate specificity. *RNA*. 1998;4(7):856–869. doi:10.1017/S1355838298980396
29. Behm-Ansmant I, Massenet S, Immel F, Patton JR, Motorin Y, Branlant C. A previously unidentified activity of yeast and mouse RNA: pseudouridinesynthases 1 (Pus1p) on tRNAs. *RNA*. 2006;12(8):1583–1593. doi:10.1261/rna.100806
30. Carlile TM, Rojas-Duran MF, Zinshteyn B, Shin H, Bartoli KM, Gilbert WV. Pseudouridine profiling reveals regulated mRNA pseudouridylation in yeast and human cells. *Nature*. 2014;515(7525):143–146. doi:10.1038/nature13802
31. Martinez NM, Su A, Burns MC, et al. Pseudouridine synthases modify human pre-mRNA co-transcriptionally and affect pre-mRNA processing. *Mol Cell*. 2022;82(3):645–659 e649. doi:10.1016/j.molcel.2021.12.023
32. Zhao X, Patton JR, Davis SL, Florence B, Ames SJ, Spanjaard RA. Regulation of nuclear receptor activity by a pseudouridine synthase through posttranscriptional modification of steroid receptor RNA activator. *Mol Cell*. 2004;15(4):549–558. doi:10.1016/j.molcel.2004.06.044
33. Komili S, Silver PA. Coupling and coordination in gene expression processes: a systems biology view. *Nat Rev Genet*. 2008;9(1):38–48. doi:10.1038/nrg2223
34. van Dam S, Vosa U, van der Graaf A, Franke L, de Magalhaes JP. Gene co-expression analysis for functional classification and gene-disease predictions. *Brief Bioinform*. 2018;19(4):575–592. doi:10.1093/bib/bbw139
35. Rui L. Energy metabolism in the liver. *Compr Physiol*. 2014;4(1):177–197.
36. Boese AC, Kang S. Mitochondrial metabolism-mediated redox regulation in cancer progression. *Redox Biol*. 2021;42:101870. doi:10.1016/j.redox.2021.101870
37. Kwon SM, Lee YK, Min S, Woo HG, Wang HJ, Yoon G. Mitoribosome defect in hepatocellular carcinoma promotes an aggressive phenotype with suppressed immune reaction. *iScience*. 2020;23(6):101247. doi:10.1016/j.isci.2020.101247
38. Lee HY, Nga HT, Tian J, Yi HS. Mitochondrial metabolic signatures in hepatocellular carcinoma. *Cells*. 2021;10:8.
39. Tuli HS, Kaur J, Vashishth K, et al. Molecular mechanisms behind ROS regulation in cancer: a balancing act between augmented tumorigenesis and cell apoptosis. *Arch Toxicol*. 2023;97(1):103–120. doi:10.1007/s00204-022-03421-z
40. Liang JQ, Teoh N, Xu L, et al. Dietary cholesterol promotes steatohepatitis related hepatocellular carcinoma through dysregulated metabolism and calcium signaling. *Nat Commun*. 2018;9(1):4490. doi:10.1038/s41467-018-06931-6
41. Adams LA, Lymp JF, St Sauver J, et al. The natural history of nonalcoholic fatty liver disease: a population-based cohort study. *Gastroenterology*. 2005;129(1):113–121. doi:10.1053/j.gastro.2005.04.014
42. Day CP, James OF. Steatohepatitis: a tale of two "hits"? *Gastroenterology*. 1998;114(4):842–845. doi:10.1016/S0016-5085(98)70599-2
43. Takaki A, Kawai D, Yamamoto K. Multiple hits, including oxidative stress, as pathogenesis and treatment target in non-alcoholic steatohepatitis (NASH). *Int J Mol Sci*. 2013;14(10):20704–20728. doi:10.3390/ijms141020704
44. Dimri M, Satyanarayana A. Molecular signaling pathways and therapeutic targets in hepatocellular carcinoma. *Cancers*. 2020;12(2):491. doi:10.3390/cancers12020491
45. He G, Karin M. NF-kappaB and STAT3 - key players in liver inflammation and cancer. *Cell Res*. 2011;21(1):159–168. doi:10.1038/cr.2010.183
46. Yang YM, Kim SY, Seki E. Inflammation and liver cancer: molecular mechanisms and therapeutic targets. *Semin Liver Dis*. 2019;39(1):26–42. doi:10.1055/s-0038-1676806
47. Liu P, Ge M, Hu J, et al. A functional mammalian target of rapamycin complex 1 signaling is indispensable for c-Myc-driven hepatocarcinogenesis. *Hepatology*. 2017;66(1):167–181. doi:10.1002/hep.29183
48. Xin B, Yamamoto M, Fujii K, et al. Critical role of Myc activation in mouse hepatocarcinogenesis induced by the activation of AKT and RAS pathways. *Oncogene*. 2017;36(36):5087–5097. doi:10.1038/onc.2017.114

49. Wang H, Wang P, Xu M, et al. Distinct functions of transforming growth factor-beta signaling in c-MYC driven hepatocellular carcinoma initiation and progression. *Cell Death Dis*. 2021;12(2):200. doi:10.1038/s41419-021-03488-z
50. Rufini A, Tucci P, Celardo I, Melino G. Senescence and aging: the critical roles of p53. *Oncogene*. 2013;32(43):5129–5143. doi:10.1038/onc.2012.640
51. Kan G, Wang Z, Sheng C, et al. Dual inhibition of DKC1 and MEK1/2 synergistically restrains the growth of colorectal cancer cells. *Adv Sci*. 2021;8(10):2004344. doi:10.1002/advs.202004344
52. Song D, Guo M, Xu S, et al. HSP90-dependent PUS7 overexpression facilitates the metastasis of colorectal cancer cells by regulating LASP1 abundance. *J Exp Clin Cancer Res*. 2021;40(1):170. doi:10.1186/s13046-021-01951-5